



# Double-metal cyanide-supported Pd catalysts for highly efficient hydrogenative ring-rearrangement of biomass-derived furanic aldehydes to cyclopentanone compounds

Xiang Li<sup>a,b,1</sup>, Qiang Deng<sup>a,b,\*,1</sup>, Shihong Zhou<sup>a,b</sup>, Jiedong Zou<sup>a,b</sup>, Jun Wang<sup>a,b</sup>, Rong Wang<sup>a,b</sup>, Zheling Zeng<sup>a,b</sup>, Shuguang Deng<sup>a,b,c,\*</sup>

<sup>a</sup> Key Laboratory of Poyang Lake Environment and Resource Utilization, Nanchang University, Ministry of Education, Nanchang 330031, PR China

<sup>b</sup> School of Resource, Environmental and Chemical Engineering, Nanchang University, Nanchang 330031, PR China

<sup>c</sup> School for Engineering of Matter, Transport and Energy, Arizona State University, 551 E. Tyler Mall, Tempe, AZ 85287, USA

## ARTICLE INFO

### Article history:

Received 29 January 2019

Revised 16 August 2019

Accepted 22 August 2019

### Keywords:

Furanic aldehydes

Pd/DMC

Hydrogenative ring-rearrangement

Cyclopentanone compounds

High-value chemicals

## ABSTRACT

The hydrogenative ring-rearrangement of biomass-derived furanic aldehydes (furfural or 5-hydroxymethyl furfural) to cyclopentanone compounds (cyclopentanone or 3-hydroxymethyl cyclopentanone) is of great significance for high-value chemicals. The Brønsted acid in metal-support bifunctional catalysts causes a serious carbon loss, and the weak Lewis acid is difficult to induce hydrolysis reaction steps. Here, a double-metal cyanide (DMC) catalyst with pure moderate Lewis acid sites was investigated for solving the above problems. The crystal structure and the Lewis acidity of the catalyst are controlled by different kinds of metals, and the surface properties are changed by a complexing effect. Pd clusters of 8 nm are uniformly dispersed on the surface after impregnation on the double-metal cyanide. For the reaction of furanic aldehydes, the Pd/FeZn-DMC catalyst with a moderate Lewis acidity shows a high efficiency for the synthesis of cyclopentanone compounds, whereas the Pd/FeNi-DMC and Pd/FeCo-DMC catalysts with a weak Lewis acidity result in a yield above 90.2% of furanic alcohols (furfuryl alcohol or 2,5-bis(hydroxymethyl)furan). The catalytic activity of Pd/FeZn-DMC is controlled by the surface area based on the accessibility of the Lewis acid sites, and the highest yields of 96.6% and 87.5% are obtained for cyclopentanone and 3-hydroxymethyl cyclopentanone, respectively. Furthermore, the catalyst is resistant to leaching and performs stably after 6 runs. This study not only provides a promising route for efficient production of cyclopentanone compounds but also shows the excellent advantage of DMC-based bifunctional catalysis in biomass conversion reactions.

© 2019 Elsevier Inc. All rights reserved.

## 1. Introduction

Cyclopentanone compounds (cyclopentanone or 3-hydroxymethyl cyclopentanone) are important intermediates for fine chemicals, which can be used for the synthesis of medicines, spices, pesticides, dyes, rubber and high-density fuels [1,2]. Currently, cyclopentanone is mainly synthesized from the decarboxylation cyclization of petroleum-derived adipic acid [3]. However, 3-hydroxymethyl cyclopentanone has not been industrially synthesized from petroleum-derived chemicals yet. To reduce

the excessive dependence on petroleum and extend the application of biomass, the synthesis of biomass-based fine chemicals has attracted great attention [4,5]. Lignocellulose, the most abundant organic substance in nature, can be transformed into biomass platform furanic aldehydes (furfural or 5-hydroxymethyl furfural), which play an important role in the catalytic conversion of biomass.

Recently, the hydrogenative ring-rearrangement of furanic aldehydes to cyclopentanone compounds was widely reported under Group VIII or IB metal supported bifunctional catalysts in aqueous solutions, and the whole reactions were through C=O hydrogenation, furan ring hydrolysis, C=C hydrogenation, intramolecular aldol, and dehydration reaction steps [6,7]. It is confirmed that Lewis acids have a crucial effect on the hydrogenative ring-rearrangement reaction by promoting the hydrolysis and intramolecular aldol steps, but Brønsted acids easily promote the intermolecular C–C bond reaction of intermediates, leading to

\* Corresponding authors at: Key Laboratory of Poyang Lake Environment and Resource Utilization, Nanchang University, Ministry of Education, Nanchang 330031, PR China.

E-mail addresses: [dengqiang@ncu.edu.cn](mailto:dengqiang@ncu.edu.cn) (Q. Deng), [Shuguang.Deng@asu.edu](mailto:Shuguang.Deng@asu.edu) (S. Deng).

<sup>1</sup> These authors contributed equally to this work.

the production of humins [8]. Up to now, many acidic materials, such as acidic metal oxides (including  $\text{TiO}_2$ ,  $\text{ZnO}$ ,  $\text{Co}_3\text{O}_4$ ,  $\text{Al}_2\text{O}_3$ ) and acidic molecular sieves (including HY, HZSM-5, SBA-15), were used as supports for the furfural reaction [1,9–15]. Meanwhile, unlike furfural, a stronger acidic support ( $\text{Ta}_2\text{O}_5$ ,  $\text{Nb}_2\text{O}_5$ ) is needed for 5-hydroxymethyl furfural because its hydrogenation intermediate 2,5-bis(hydroxymethyl)furan is more difficult to hydrolyze because of the electron withdrawing hydroxymethyl group [16–18]. Unfortunately, under the coexisting action of Lewis and Brønsted acids on the traditional supports, the synthesis efficiency of cyclopentanone compounds is unsatisfactory, because a large amount of intermediates (furfuryl alcohol or 2,5-bis(hydroxymethyl)furan) and low-value humins are generated. It has been reported that the pure Lewis acidic Cr-MIL-101-based catalyst completely prevents the generation of humins and shows a considerable yield of cyclopentanone over 60% from furfural [19]. However, because of the weak Lewis acidity of the unsaturated coordination of  $\text{Cr}^{3+}$  ions, it can only catalyze 5-hydroxymethyl furfural to 2,5-bis(hydroxymethyl)tetrahydrofuran, and cannot further open the furan ring and trigger the synthesis of 3-hydroxymethyl cyclopentanone [19]. Therefore, to efficiently synthesize cyclopentanone compounds, the synthesis of pure moderate Lewis acidity materials as the support is important.

Double-metal cyanides (DMCs), famous for Prussian blue, are constructed by octahedral metal cyanide anion groups bridged with metal ions through a cyanide group ( $\text{C}\equiv\text{N}$ ). It is safe for human health.[20] It shows wide prospects in adsorption [21], energy storage [22], biomedicine [23] and catalysis [24,25]. Usually, triblock copolymers as a complexing agent were added in the synthesis process to suppress overgeneration and thus adjust the surface area. Meanwhile, the structure of DMCs can be easily controlled by different metals. For instance, FeZn-DMC is prone to having a rhombohedral lattice structure with an R-3c space group. However, FeNi-DMC and FeCu-DMC have a cubic structure with an Fm3m space group although the synthesis conditions are the same [26]. On the inner and outer surface edges of a DMC crystal, the coordination unsaturated vacancy  $\text{M}^{2+}$  ions can be used as Lewis acid sites. At present, as a monofunctional Lewis acidic catalyst, DMCs are mainly used to catalyze polymerization [27], esterification [28], transesterification [28,29], polyesterification [30], hydroamination [31], Prins condensation [32] and oxidation reactions [33]. Especially, they have industrial applications on the polymerization of epoxides based on their high activity, stability and low price. To the best of our knowledge, DMCs have not been reported in the field of bifunctional catalysis up to now.

Here, we focus on Lewis acidic DMC-supported Pd nanoparticle bifunctional catalysts as a highly efficient catalyst for the hydrogenative ring-rearrangement of furanic aldehydes. These catalysts show a controllable Lewis acidity and surface by adjusting the structure and the amount of the complexing agent. As a result, the Pd/FeZn-DMC catalysts show a higher activity and selectivity to cyclopentanone compounds than traditional catalysts, which is attributed to the appropriate Pd particle size, pure moderate Lewis acidity, and suitable accessibility of active sites. Moreover, it is highly stable against leaching and shows an unchanged performance after six runs. The DMC-based bifunctional catalysis is promising in the catalytic transformation of biomass derivatives.

## 2. Experimental

### 2.1. Materials

Furfural (99.5%), N,N-dimethyl formamide, ethanol, potassium hexacyanoferrate(II) ( $\text{K}_4[\text{Fe}(\text{CN})_6]\cdot 3\text{H}_2\text{O}$ ), zinc chloride ( $\text{ZnCl}_2$ ),

nickel chloride ( $\text{NiCl}_2\cdot 6\text{H}_2\text{O}$ ) and cobalt chloride ( $\text{CoCl}_2\cdot 6\text{H}_2\text{O}$ ), *tert*-butanol, palladium chloride ( $\text{PdCl}_2$ ),  $\text{TiO}_2$ ,  $\text{Nb}_2\text{O}_5$ , and  $\text{Al}_2\text{O}_3$  were purchased from Sinopharm Chemical Reagent Company. 5-Hydroxymethyl furfural (99%) was obtained from Beijing Coupling Technology Company. Poly(ethyleneglycol)-block-poly(propylene glycol)-block-poly(ethylene glycol) ( $\text{P}_{123}$ , average molecular weight = 5800) was purchased from Sigma-Aldrich. All chemicals were used without further purification. H $\beta$  ( $\text{SiO}_2/\text{Al}_2\text{O}_3 = 25$ ) supplied by Tianjin Nankai Catalysts Company was calcined in air for 6 h at 550 °C. Al-MCM-41 ( $\text{SiO}_2/\text{Al}_2\text{O}_3 = 26.8$ ) and Cr-MIL-101 were synthesized according to previous studies [2,34].

### 2.2. Synthesis of catalysts

FeZn DMC was synthesized by a simple precipitation method. A mixture of 0.1 mol  $\text{ZnCl}_2$ , 20 mL water and 20 mL *tert*-butanol was added to 40 mL 0.25 mol/L  $\text{K}_4\text{Fe}(\text{CN})_6\cdot 3\text{H}_2\text{O}$  aqueous solution slowly over 1 h at 50 °C under vigorous stirring. Then, quantitative amounts of  $\text{P}_{123}$  in 2 mL water and 40 mL *tert*-butanol were added over 10 min and stirred continuously for 1 h. Subsequently, the solid was centrifuged and washed with water to remove the uncompleted ions and complexing agent, followed by drying at 60 °C for 8 h. The amounts of  $\text{P}_{123}$  were 0, 5, 10, and 15 g, and the resultant white solids were labeled FeZn-0, FeZn-5, FeZn-10, and FeZn-15, respectively. As a comparison, some small particles of FeZn-0 were ball-milled in an agate grinding jar for 30 min and labeled FeZn-0B. Similarly, dark green FeCo and green FeNi solids were synthesized with 15 g  $\text{P}_{123}$  by changing  $\text{ZnCl}_2$  to  $\text{NiCl}_2\cdot 6\text{H}_2\text{O}$  and  $\text{CoCl}_2\cdot 6\text{H}_2\text{O}$  and labeled FeNi-15 and FeCo-15, respectively.

A series of supported Pd catalysts was prepared by the incipient wetness impregnation method. Typically, given amounts of  $\text{PdCl}_2$  and 1 g DMC were added to 10 mL water, thoroughly mixed, and dried at 80 °C over a rotary evaporator. The solid was recovered, dried at 100 °C for 6 h, and reduced in a quartz tube furnace at 300 °C for 3 h under a gas mixture of 10%  $\text{H}_2/90\%$   $\text{N}_2$ . If not mentioned, the Pd loading is 5 wt%.

### 2.3. Catalyst characterizations

The crystal structures of the catalysts were studied by powder X-ray diffraction (XRD) using a PANalytical Empyrean diffractometer with Cu-K $\alpha$  radiation. The pore textural properties were measured by  $\text{N}_2$  adsorption-desorption at  $-196$  °C on an ASAP 2046 surface analyzer. The specific surface area was calculated by the BET method. Morphologies were obtained with a JSM-6701F scanning electron microscope and a JEM-2100 transmission electron microscope. Acid properties were analyzed by the infrared spectroscopy of adsorbed pyridine using a Bruker VERTEX 70 spectrometer. For the IR analysis, self-supported wafers (10 mg/cm<sup>2</sup>) were degassed for 1 h under vacuum at 200 °C, then the adsorption of pyridine proceeded at 60 °C for 30 min followed by desorption at 150 °C and 250 °C for 20 min, and the transmission spectra were recorded. Elemental analysis was carried out using Inductively Coupled Plasma Optical Emission Spectrometry on a PerkinElmer Optima 8000 spectrometer. The thermal stabilities were analyzed by thermal gravimetric analysis on a NETZSCH-STA 2500 instrument in a  $\text{N}_2$  atmosphere.

### 2.4. Catalytic reactions

The catalytic reactions were carried out in a 100 mL batch autoclave (Parr Instrument) equipped with mechanical stirring. Typically, a mixture of furanic aldehydes (10.4 mmol) and water (40 mL) and 0.1 g catalyst were added to the autoclave, then reacted under 4.0 MPa  $\text{H}_2$  at 150 °C and sampled periodically. Then,

a certain amount of N,N-dimethyl formamide was added as an internal standard substance. The products were analyzed by an Agilent 6890 N GC/5973 MS detector and quantified by a Trace 1300 gas chromatograph equipped with an FID detector and a TG-WAXMS capillary column (30 m × 0.32 mm). The reported data were the mean values of three trials with small error bars.

### 3. Results and discussion

#### 3.1. Structural characteristics of Pd/DMC

Fig. 1A shows the XRD patterns of the DMC. It is found that the DMC is consistent with the uniform  $K_2M_3[Fe(CN)_6]_2$  ( $M = Zn^{2+}, Ni^{2+}, Co^{2+}$ ) structure type, which suggests that FeZn has an R-3c space group structure in which  $Zn^{2+}$  is tetra-coordinated connecting with four  $N\equiv C$  bonds. Differently, FeNi and FeCo have an Fm3m space structure, and Ni/Co is hexa-coordinated connecting with four  $N\equiv C$  bonds and two water molecules, which is in good agreement with the reported results [35,36]. The addition of  $P_{123}$  reduces the crystalline intensity slightly, because the complexing agent prevents the DMC from growing largely. However, the ball-milled sample FeZn-0B has greatly destroyed the crystalline structure by reducing the crystal particle size. After impregnation, the XRD patterns are almost identical to the pure DMC, confirming the well preservation of the DMC structure after the incorporation of Pd (Fig. 1B).

Elemental analysis shows the Pd content on Pd/DMC catalysts is 5.0 wt% via the impregnation method (Table 1). The Zn:Fe molar ratio is 1.57:1 for Pd/FeZn-0, meaning that the Zn:Fe ratio is slightly higher than the stoichiometrically expected 1.5. Because of the excess of  $Zn^{2+}$  in the synthesis mixture, it is indicated that zinc terminates the crystals and is abundant on the outer surface. Meanwhile, the addition of  $P_{123}$  suppresses overgeneration and increases Zn:Fe molar ratio from 1.57 to 1.80 for Pd/FeZn [31].

Fig. 2 shows the  $N_2$  adsorption-desorption isotherms of Pd/DMC catalysts. Pd/FeZn-0 shows a type II adsorption-desorption isotherm, and Pd/FeZn-5, 10, and 15 slightly show a type IV isotherm,

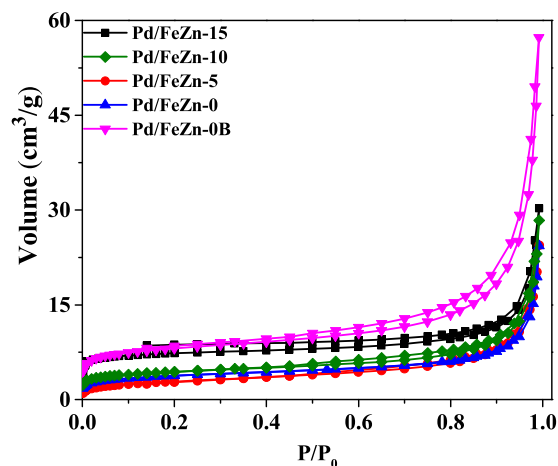


Fig. 2.  $N_2$  adsorption isotherms of Pd/DMC.

indicating the existence of mesopores after introducing the organic complexing agents. The controllable BET surface area, pore volume and pore size range from 10.3 to 26.8  $m^2/g$ , 0.034 to 0.040  $cm^3/g$ , and 18.0 to 24.2 nm, respectively, for Pd/FeZn-0 to Pd/FeZn-15 by adjusting the amount of  $P_{123}$  (Table 1). Meanwhile, the simple ball-milled Pd/FeZn-0B also shows a type IV isotherm with a BET surface of 27.6  $m^2/g$  by decreasing the crystal particle size. Cubic FeNi-15 and FeCo-15 have a larger BET surface of 85.2 and 75.3  $m^2/g$ , respectively (Fig. S1).

The SEM image shows that the DMC has very uniformly sized particles of 1–2  $\mu m$ , and the particle size did not change by adding complexing agents (Fig. 3A–C), except for the ball-milled sample Pd/FeZn-0B with a smaller size. The presence of well dispersed Pd nanoparticles of approximately 8 nm was observed on the surface of the FeZn-DMC host, without any aggregation (Fig. 3D–F). The FeNi-DMC and FeCo-DMC show Pd nanoparticles of about 9 nm. As a comparison, other acidic materials supported Pd (Pd/C, Pd/H $\beta$ , Pd/Al-MCM-41, Pd/Al $_2$ O $_3$ , Pd/Nb $_2$ O $_5$ , Pd/TiO $_2$ , Pd/MIL-

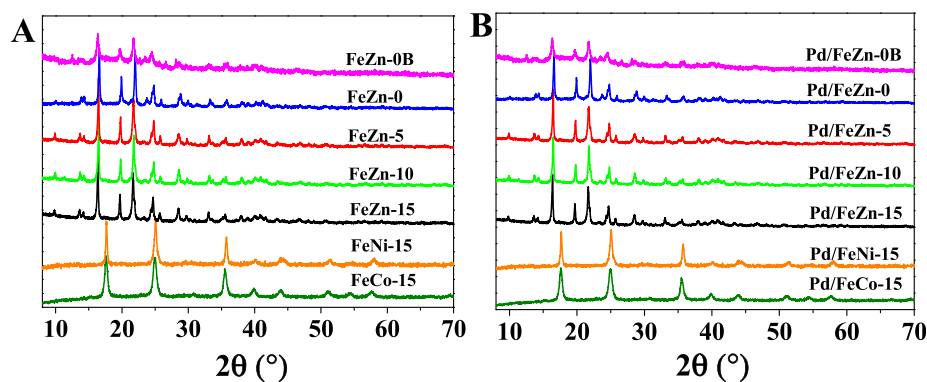


Fig. 1. X-ray diffraction patterns of (A) DMC and (B) Pd/DMC.

Table 1

Physical properties of the synthesized catalysts. a: after 6 catalytic runs.

Samples	$S_{BET}$ ( $m^2/g$ )	Pore volume ( $cm^3/g$ )	Pore Size (nm)	Zn:Fe (molar ratio)	Pd content (wt%)
Pd/FeZn-0B	27.6	0.081	24.9	1.62:1	4.98
Pd/FeZn-0	10.3	0.036	18.0	1.57:1	4.96
Pd/FeZn-5	13.2	0.034	19.1	1.65:1	5.01
Pd/FeZn-10	14.9	0.038	20.8	1.73:1	4.97
Pd/FeZn-15	26.8	0.040	24.2	1.80:1	4.95
Pd/FeZn-15 <sup>a</sup>	18.6	0.038	21.6	1.75:1	4.93

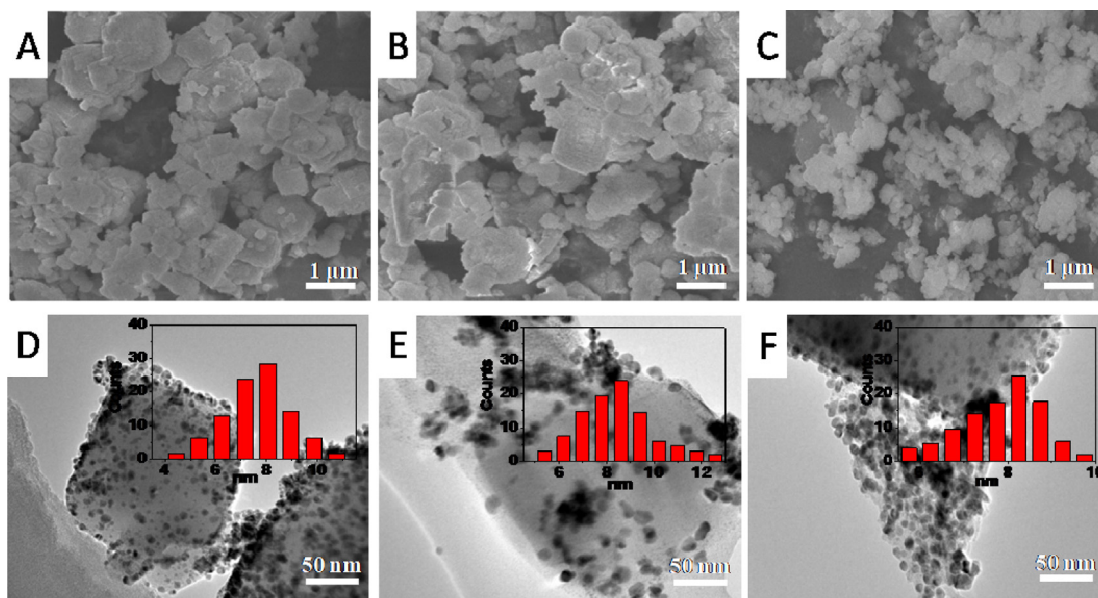


Fig. 3. SEM and TEM micrographs of (A) FeZn-0, (B) FeZn-15, (C) FeZn-0B, (D) Pd/FeZn-15, (E) Pd/FeNi-15 and (F) Pd/FeCo-15.

101) shows smaller Pd nanoparticles ranged from 3 to 6 nm (Fig. S2). As shown in Fig. S3, pyridine-adsorbed FTIR spectra were used to detect the acid sites. Adsorption peaks are observed at  $1450\text{ cm}^{-1}$  for all the samples. Meanwhile, no peaks are observed at  $1540\text{ cm}^{-1}$ . This confirms a pure Lewis support without any Brønsted acids. Notably, the area of the most intensive peak ( $1450\text{ cm}^{-1}$ ) is well associated with the BET surface area for the sample treated at  $150\text{ }^{\circ}\text{C}$  (Fig. 4), with Pd/FeZn-0 at  $150\text{ }^{\circ}\text{C}$  as a baseline, because a larger area is more likely to expose more acid sites that adsorb more pyridine [30]. However, at the higher adsorption temperature ( $250\text{ }^{\circ}\text{C}$ ), due to the strong Lewis acidity in the catalyst, the signal of Pd/FeZn is higher than that of Pd/FeCo and Pd/FeNi, showing a stronger Lewis acidity of tetra-coordinated unsaturated  $\text{Zn}^{2+}$ . Meanwhile, with the increase in desorption temperatures, the amount of the adsorbed pyridine in all Pd/FeZn samples was synchronously decreased, showing that the introduction of  $\text{P}_{123}$  only expands the internal structure of particles and cannot influence their Lewis acidity. Meanwhile, as shown in Fig. S4, the acidic molecular sieves (H $\beta$ , Al-MCM-41) show both Lewis and Brønsted acidity.

The thermal stability of Pd/DMC (Fig. S5) shows that the weight decreased from  $60\text{ }^{\circ}\text{C}$  to  $200\text{ }^{\circ}\text{C}$  by the loss of crystal and noncrystal water. Pd/DMC retains its structure at  $300\text{ }^{\circ}\text{C}$ , indicating that it has a great stability under severe reaction conditions.

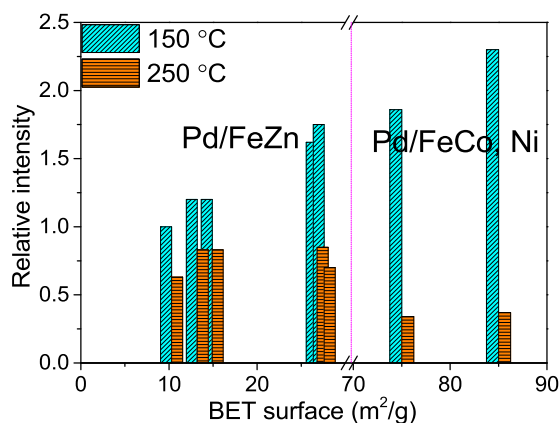
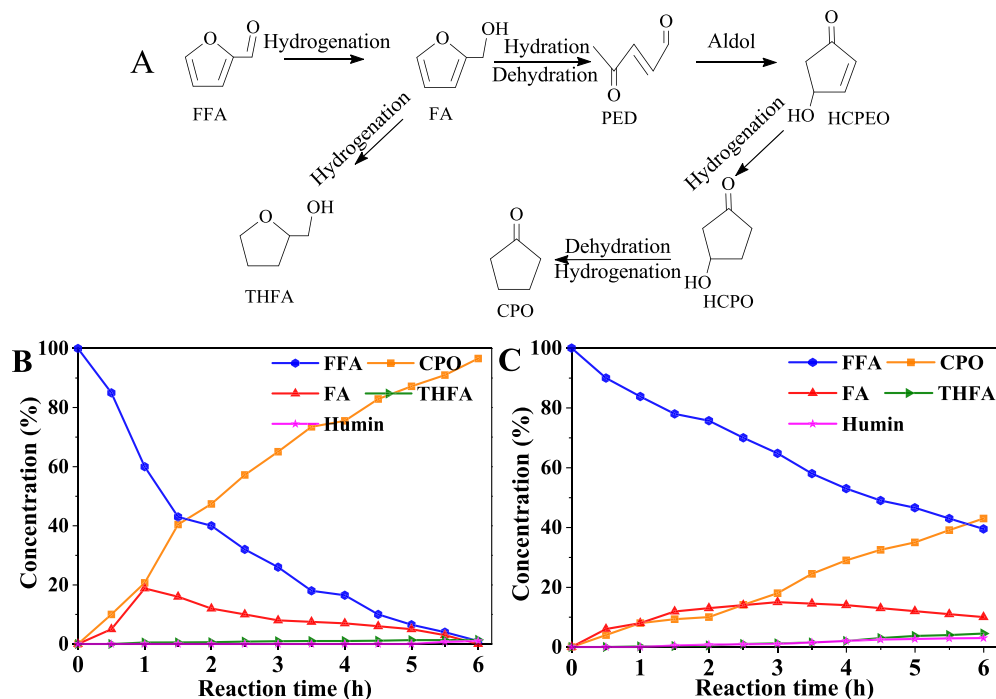


Fig. 4. Relation between the intensity of the  $1450\text{ cm}^{-1}$  peak and the BET surface.

### 3.2. Hydrogenative ring-rearrangement of furfural to cyclopentanone

As shown in Fig. 5A, furfural (FFA) was first converted to furfuryl alcohol (FA) by C=O hydrogenation at the beginning, then acid-catalytically hydrolyzed to form 2-pentene-1,4-dione (PED) at the acid sites of the catalysts, and further generated 3-hydroxycyclopentanone (HCPO) via acid-catalytic conversion of an intramolecular aldol intermediate 4-hydroxy-2-cyclopentenone (HCPEO) in a subsequent C=C hydrogenation reaction. Finally, cyclopentanone (CPO) is obtained by dehydration in a subsequent C=C hydrogenation reaction. The fact that trace amounts of PED, HCPEO and HCPO are detected in gas chromatograph confirms the reaction mechanism. Meanwhile, it also shows that the intramolecular aldol, C=C hydrogenation, and dehydration reactions occurred quickly. Apart from the main reaction pathway, there are some side reactions, including the excessive hydrogenation of FFA to form tetrahydrofurfuryl alcohol (THFA) and the intermolecular C—C bonding reaction of intermediates to form humins. Pd/DMC only shows a high hydrogenation activity of furfural, but a low activity of hydrolyzing the furan ring. However, FeZn-DMC does not have the catalytic activity for furfural. It confirms that noble metals and acid supports play respective roles in this reaction (Fig. 6A). To promote the hydrogenation reaction, the Pd loading is optimized, and a satisfactory activity is achieved on a catalyst with 5 wt% Pd (Fig. S6). Fig. 5B and C show the time-dependent product distribution over Pd/FeZn-15 and Pd/MIL-101. Although the surface area of Pd/DMC is much lower than that of Pd/MIL-101, it shows three obvious advantages over Pd/MIL-101 in this reaction. First, the hydrogenation of C=O accelerated significantly with the conversion of FFA, increasing from 60.5% to 99.9% within 6 h, because Pd with a uniform appropriate particle size on the surface of the host is easily accessible by the reactants. Second, a stronger Lewis acidity of the DMC can greatly promote the hydrolysis of FA, with the yield of FA decreasing from 10.0% to 0.0%. Third, the hydrogenation of the furan ring is almost completely inhibited with the yield of THFA decreasing from 4.5% to 1.4%, because FA is quickly consumed and Pd with an appropriate particle size is not conducive to the hydrogenation of the furan ring [37,38].

Fig. 6A further compares the conversion and selectivity for this reaction with several reported supports. Zeolite-based Pd/H $\beta$  and



**Fig. 5.** The reaction pathway scheme (A) and the product distribution of FFA hydrogenative ring-rearrangement using Pd/FeZn-15 (B) and Pd/MIL-101 (C). Reaction conditions: FFA (10.4 mmol), catalyst (0.1 g), water (40 mL), temperature 150 °C, 4.0 MPa H<sub>2</sub>.

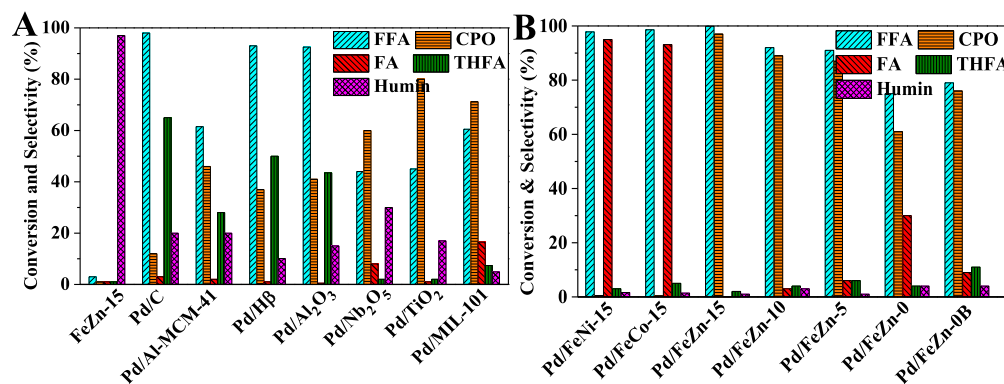


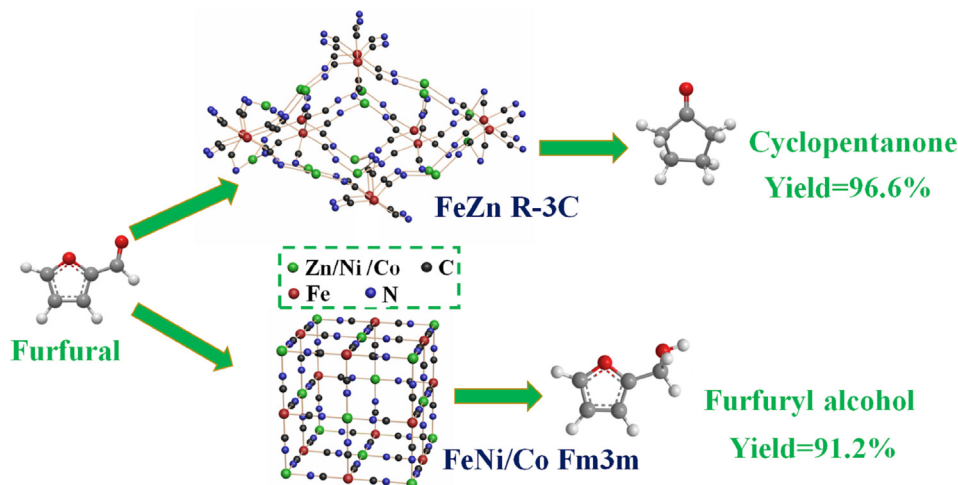
**Fig. 6.** Hydrogenative ring-rearrangement of FFA to CPO over various often-used catalysts (A) and (B) Pd/DMC. Reaction conditions: FFA (10.4 mmol), catalyst 0.1 g, water (40 mL), temperature 150 °C, 4.0 MPa H<sub>2</sub>, time 6 h.

Pd/Al-MCM-41 show a considerable activity of furfural hydrogenation. However, THFA is generated largely, because Pd with a small particle size prefers to promote the furan ring hydrogenation, and the selectivity of cyclopentanone is approximately 40% [37,38]. Additionally, considerable humins are generated via the Brønsted acid catalysis [8]. Pd/Al<sub>2</sub>O<sub>3</sub> also mainly generates THFA and humins by Pd with a small particle size and the Brønsted acid catalysis [8,39]. Comparatively, although the humins cannot be avoided completely, Pd/Nb<sub>2</sub>O<sub>5</sub> and Pd/TiO<sub>2</sub> have a higher selectivity to CPO due to their more Lewis acid sites. Pd/MIL-101 shows a higher selectivity of cyclopentanone based on the pure Lewis acidity. However, its activity is low, because the Pd particle and the Lewis acid sites are located in the framework of MIL-101, and hardly accessible to the reactants [40]. These results indicate that the selective synthesis of cyclopentanone is a challenge.

Fig. 6B shows the catalytic effect of DMC-based catalysts. Interestingly, Pd/FeNi and Pd/FeCo exhibited a high furfural conversion above 98.0% with a high selectivity toward furfuryl alcohol above 93.1% within 6 h, demonstrating that furfuryl alcohol was difficult

to be hydrolyzed with weak Lewis acidic sites. It is worth mentioning that FA cannot be transformed to THFA via furan ring hydrogenation because Pd with an appropriate particle size in the catalyst is hard to adsorb and convert the furan ring [37,38]. In contrast, Pd/FeZn with a medium-strength Lewis acidity shows a highly efficient effect of furan ring opening and a high selectivity for cyclopentanone (Scheme 1). In addition, the activity is increased with the surface area of Pd/FeZn, due to the more efficient accessibility of Lewis acid sites. At last, 99.9% conversion of furfural and 96.6% selectivity of cyclopentanone were obtained with Pd/FeZn-15. Indeed, Pd/FeZn-0B shows a higher activity and selectivity than Pd/FeZn-0 by increasing the surface area, but lower ones than Pd/FeZn-15 due to the destruction of the crystal structure.

To clearly clarify the performance of Pd/DMC, kinetic studies about the hydrogenation step of FFA and the hydrolysis step of FA are carried out. For the hydrogenation study, the  $\ln(C/C_0)$  of FFA against time gives good straight-line plots, which reveals that the hydrogenation step of FFA followed pseudo first-order kinetics (Fig. S7). Pd/DMC (Pd/FeZn, Pd/FeNi and Pd/FeCo) shows obviously



**Scheme 1.** Highly oriented synthesis of cyclopentanone and furfuryl alcohol via different catalysts.

higher kinetic parameters among all catalysts. For the hydrolysis study, to eliminate the influence of furan ring hydrogenation, the reaction is conducted without hydrogen. Pd/FeZn shows the highest kinetic parameters, whereas Pd/FeCo and Pd/FeNi are inactive. These results clearly show that the excellent catalytic efficiency of Pd/FeZn is ascribable to two advantages in the two steps.

### 3.3. Hydrogenative ring-rearrangement of 5-hydroxymethyl furfural to 3-hydroxymethyl cyclopentanone

Similar to furfural, 5-hydroxymethyl furfural generates 2,5-bis(hydroxymethyl)furan (BHF) and 1-hydroxy-3-hexene-2,5-dione (HHED) via C=O hydrogenation and hydrolysis reactions.

Differently, the hydrogenation of HHED occurs to form the intermediate HHD first, and then HHCPN is produced by the intramolecular aldol reaction of HHD, which is transformed to HCPN finally. 2,5-Bis(hydroxymethyl)tetrahydrofuran (THBHF) was also generated by the excessive hydrogenation, as shown in Fig. 7A. Trace amounts of HHED and HHCPN were detected in these reactions, indicating that the C=C hydrogenation and dehydration reactions are fast, as discussed above. Unlike furfural, many intermediates BHF and HHD are detected in the 5-hydroxymethyl furfural reaction because the hydroxymethyl group transfers electrons to the furan ring or the carbonyl group, thus reducing the reactivity of BHF and HHD (Fig. 7B, C). Moreover, the hydroxymethyl group brings up the steric hindrance that also makes the reaction more

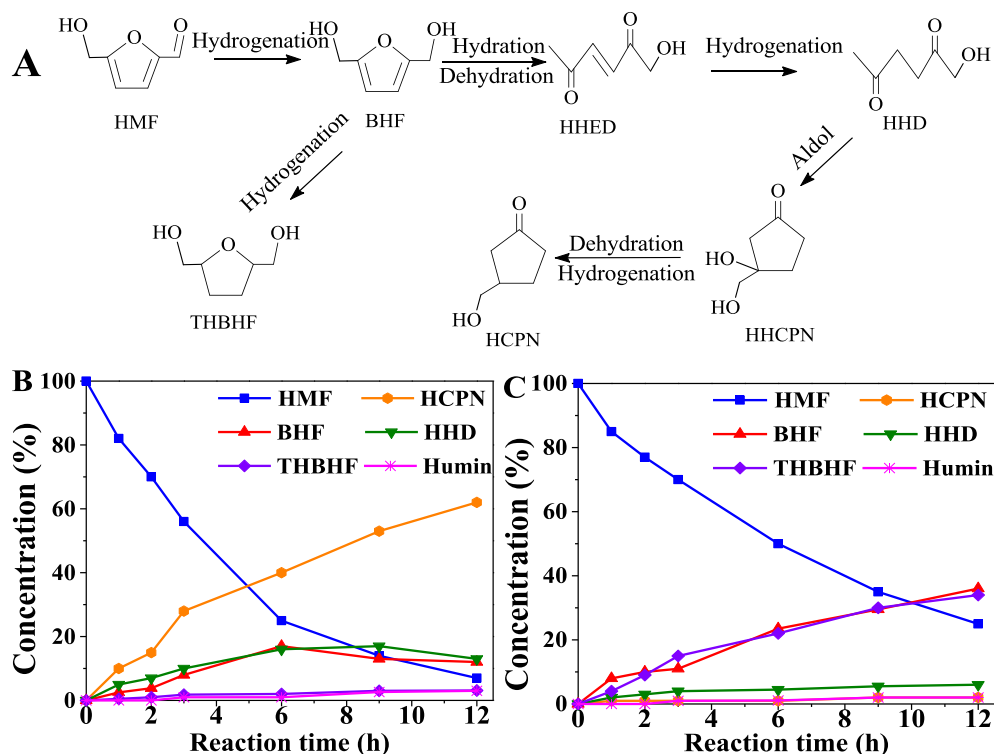


**Fig. 7.** The reaction pathway scheme (A) and the product distribution of HMF hydrogenative ring-rearrangement using Pd/FeZn-15 (B) and Pd/MIL-101 (C). Reaction conditions: FFA (10.4 mmol), catalyst (0.1 g), water (40 mL), temperature 150 °C, 4.0 MPa H<sub>2</sub>.

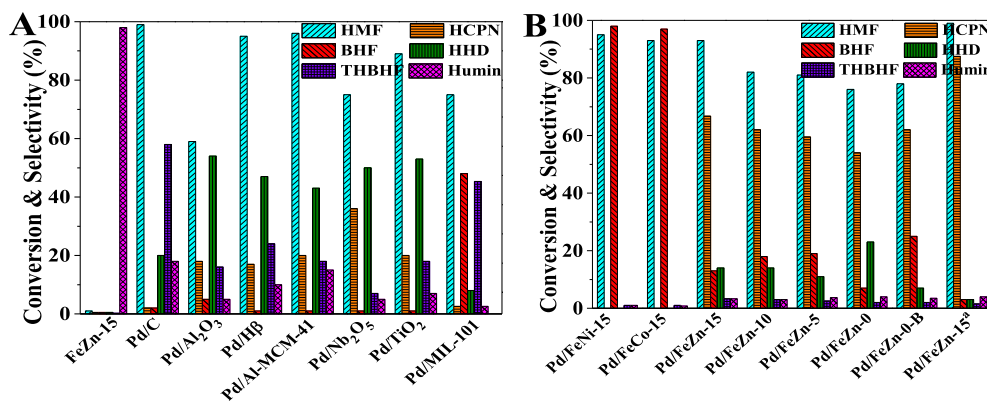


**Fig. 8.** Hydrogenative ring-rearrangement of HMF to HCPN over various often-used catalysts (A) and (B) Pd/DMC. Reaction conditions: HMF (10.4 mmol), catalyst 0.1 g, water (40 mL), temperature 150 °C, 4.0 MPa H<sub>2</sub>, time 12 h. Pd/FeZn-15<sup>a</sup> catalyst: 24 h reaction time.

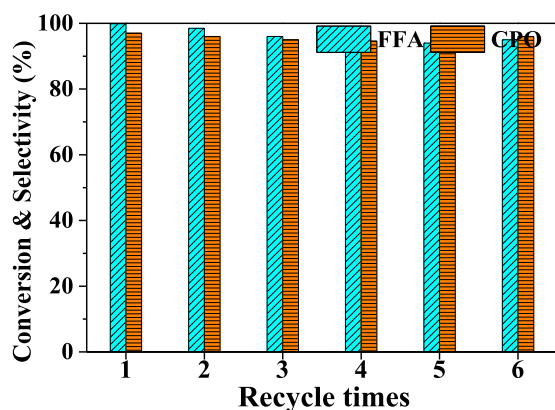


**Fig. 9.** Recycling Performance of Pd/FeZn-15 in furfural hydrogenative ring-rearrangement. Reaction conditions: HMF (10.4 mmol), Pd/FeZn-15 (0.1 g), water (40 mL), temperature 150 °C, 4.0 MPa H<sub>2</sub>, time 6 h.

difficult [41]. The transformation efficiency of HMF to HCPN is lower, so the reaction time extends to 12 h. Likewise, compared with Pd/MIL-101, Pd/DMC has a higher activity of C=O hydrogenation without any hydrogenation of the furan ring. Better yet, the DMC promotes the hydrolysis of BHF and further intramolecular aldol reaction, whereas Pd/MIL-101 with a weak Lewis acidity cannot open the furan ring and a large amount of BHF is produced. At last, the reaction upgraded the conversion of HMF, which increased from 74.9% to 93.1%, and the yield of HCPN, which increased from 2.1% to 60.2%, in 12 h by changing Pd/MIL-101 to Pd/DMC.

Fig. 8A also compares the activity of the various catalysts. Pd/Al<sub>2</sub>O<sub>3</sub>, Pd/H $\beta$  and Pd/Al-MCM-41 have a high selectivity of THBHF. Differently, Pd/Nb<sub>2</sub>O<sub>5</sub> with a higher acidity shows a higher selectivity to HCPN than weak acidic Pd/TiO<sub>2</sub>, which further confirms that a strong acidity support is important for hydrolysis and intramolecular aldol steps for the HMF reaction. Pd/MIL-101 cannot open the furan ring, and a large amount of BHF is further hydrogenated to THBHF by small Pd particles. Pd/FeNi and Pd/FeCo only show a high activity of C=O hydrogenation, and BHF yields of 93.1% and 90.2% were obtained, respectively (Fig. 8B). All FeZn-based catalysts exhibit product transformation via main reaction routes, and there is almost no other byproducts. The selectivity of HCPN is increased from 54.0% to 67.7% with the surface area of Pd/FeZn-0 to Pd/FeZn-15, because more Lewis acid sites promote HHD and BHF to be consumed via hydrolysis and intramolecular aldol reactions. In addition, after 24 h, the conversion over Pd/FeZn-15 is 99.9% with a selectivity of 87.5%.

### 3.4. Catalyst stability and recycling

A rapid, hot-catalyst filtration test was performed, and no further conversion of furfural and yield of cyclopentanone in the filtrate were found after the removal of Pd/FeZn DMC (Fig. S8), which proves the true heterogeneously catalytic nature of each reaction step and suggests the stability of Pd particles and the DMC. The recycling of Pd/DMC was further evaluated in the hydrogenative ring-rearrangement of furfural. The catalyst was centrifuged after the reaction, washed with water, and used for the next run. As shown in Fig. 9, after 6 runs, both the conversion and the selectivity still stay above 95.1%. The slight decrease of catalytic kinetic can be attributed to the decrease of specific surface area (Table 1, Fig. S9). However, the crystalline structures, Lewis acidity, and chemical compositions are well preserved in the used catalyst as evidenced by the XRD, pyridine-adsorbed FTIR and ICP-OES data (Table 1, Fig. S10, S11), showing that the catalysts are stable under the present reaction conditions.

## 4. Conclusions

A highly efficient DMC-based bifunctional catalyst is developed for the hydrogenative ring-rearrangement of biomass-derived furanic aldehydes. Various pure Lewis acidities can be obtained by different types of metals. Pd/DMC shows conversion of a much higher activity and selectivity compared with traditional reported supports. Among the catalysts studied in this work, Pd/FeZn with a moderate pure Lewis acidity shows a yield of cyclopentanone compounds over 87.5%, whereas Pd/FeNi and Pd/FeCo with a weak Lewis acidity show a yield of furanic alcohols over 90.2%. A higher conversion can be achieved with more complexing agent. In addition, Pd/DMC shows an excellent stability in recycling runs, without any obvious Pd leaching and DMC structure degradation. This study provides a promising method for the synthesis of cyclopentanone and demonstrates the new prospect for the application of DMCs as a bifunctional catalyst.

### Acknowledgements

The authors appreciate the supports from the National Natural Science Foundation of China (21878138, 21706112, 21666021), Natural Science Foundation of Jiangxi Province (20171BAB213017), Postdoctoral Science Foundation of China (2017M622104), and the “Thousand Talents Plan” of China.

### Declaration of Competing Interest

The authors declare no conflict of interest.

## Appendix A. Supplementary material

Supplementary data to this article can be found online at <https://doi.org/10.1016/j.jcat.2019.08.036>.

## References

- [1] Y. Yang, Z. Du, Y. Huang, F. Lu, F. Wang, J. Gao, J. Xu, Conversion of furfural into cyclopentanone over Ni-Cu bimetallic catalysts, *Green Chem.* 15 (2013) 1932–1940.
- [2] Q. Deng, G. Nie, L. Pan, J.-J. Zou, X. Zhang, L. Wang, Highly selective self-condensation of cyclic ketones using MOF-encapsulating phosphotungstic acid for renewable high-density fuel, *Green Chem.* 17 (2015) 4473–4481.
- [3] M. Renz, Ketone of Carboxylic acids by decarboxylation: mechanism and scope, *Eur. J. Org. Chem.* 6 (2005) 979–988.
- [4] C.O. Tuck, E. Pérez, I.T. Horváth, R.A. Sheldon, M. Poliakoff, Valorization of biomass: deriving more value from waste, *Science* 337 (2012) 695–699.
- [5] A. Berlin, No barriers to cellulose breakdown, *Science* 342 (2013) 1454–1456.
- [6] M. Hronec, K. Fulajtarová, T. Liptaj, Effect of catalyst and solvent on the furan ring rearrangement to cyclopentanone, *Appl. Catal. A: Gen.* 437–438 (2012) 104–111.
- [7] M. Hronec, K. Fulajtarová, T. Soták, Highly selective rearrangement of furfuryl alcohol to cyclopentanone, *Appl. Catal. B: Environ.* 154–155 (2014) 294–300.
- [8] T.D. Swift, H. Nguyen, Z. Erdman, J.S. Kruger, V. Nikolakis, D.G. Vlachos, Tandem Lewis acid/Brønsted acid-catalyzed conversion of carbohydrates to 5-hydroxymethylfurfural using zeolite beta, *J. Catal.* 333 (2016) 149–161.
- [9] M. Hronec, K. Fulajtarová, Selective transformation of furfural to cyclopentanone, *Catal. Commun.* 24 (2012) 100–104.
- [10] G.-S. Zhang, M.-M. Zhu, Q. Zhang, Y.-M. Liu, H.-Y. He, Y. Cao, Towards quantitative and scalable transformation of furfural to cyclopentanone with supported gold catalysts, *Green Chem.* 18 (2016) 2155–2164.
- [11] J. Guo, G. Xu, Z. Han, Y. Zhang, Y. Fu, Q. Guo, Selective conversion of furfural to cyclopentanone with CuZnAl catalysts, *ACS Sustain. Chem. Eng.* 2 (2014) 2259–2266.
- [12] X.-L. Li, J. Deng, J. Shi, T. Pan, C.-G. Yu, H.-J. Xu, Y. Fu, Selective conversion of furfural to cyclopentanone or cyclopentanol using different preparation methods of Cu-Co catalysts, *Green Chem.* 17 (2015) 1038–1046.
- [13] Y. Wang, S. Sang, W. Zhu, L. Gao, G. Xiao, CuNi@C catalysts with high activity derived from metal-organic frameworks precursor for conversion of furfural to cyclopentanone, *Chem. Eng. J.* 299 (2016) 104–111.
- [14] X. Cao, T. Lyu, W. Xie, A. Mirjalili, A. Bradicich, R. Huitema, B.W.-L. Jang, J.K. Keum, K. More, C. Liu, X. Yan, Preparation and investigation of Pd doped Cu catalysts for selective hydrogenation of acetylene, *Front. Chem. Sci. Eng.* (2019), <https://doi.org/10.1007/s11705-019-1822-3>.
- [15] C.-Y. Liu, R.-P. Wei, G.-L. Geng, M.-H. Zhou, L.-J. Gao, G.-M. Xiao, Aqueous-phase catalytic hydrogenation of furfural over Ni-bearing hierarchical Y zeolite catalysts synthesized by a facile route, *Fuel Process. Technol.* 134 (2015) 168–174.
- [16] J. Ohyama, R. Kanao, Y. Ohira, A. Satsuma, The effect of heterogeneous acid-base catalysis on conversion of 5-hydroxymethylfurfural into a cyclopentanone derivative, *Green Chem.* 18 (2016) 676–680.
- [17] J. Ohyama, R. Kanao, A. Esaki, A. Satsuma, Conversion of 5-hydroxymethylfurfural to a cyclopentanone derivative by ring rearrangement over supported Au nanoparticles, *Chem. Commun.* 50 (2014) 5633–5636.
- [18] R. Ramos, A. Grigoropoulos, N. Perret, M. Zanella, A.P. Katsoulidis, T.D. Manning, J.B. Claridge, M.J. Rosseinsky, Selective conversion of 5-hydroxymethylfurfural to cyclopentanone derivatives over Cu-Al<sub>2</sub>O<sub>3</sub> and Co-Al<sub>2</sub>O<sub>3</sub> catalysts in water, *Green Chem.* 19 (2017) 1701–1713.
- [19] R. Fang, H. Liu, R. Luque, Y. Li, Efficient and selective hydrogenation of biomass-derived furfural to cyclopentanone using Ru catalysts, *Green Chem.* 17 (2015) 4183–4188.
- [20] J. Luo, A. Sam, B. Hu, C. DeBruler, X. Wei, W. Wang, T.L. Liu, Unraveling pH dependent cycling stability of ferricyanide/ferrocyanide in redox flow batteries, *Nano Energy* 42 (2017) 215–221.
- [21] A. Takahashi, H. Tanaka, D. Parajuli, T. Nakamura, K. Minami, Y. Sugiyama, Y. Hakuta, S.-I. Ohkoshi, T. Kawamoto, Historical pigment exhibiting ammonia gas capture beyond standard adsorbents with adsorption sites of two kinds, *J. Am. Chem. Soc.* 138 (2016) 6376–6379.
- [22] D. Su, M. Cortie, H. Fan, G. Wang, Prussian blue nanocubes with an open framework structure coated with pedot as high-capacity cathodes for lithium-sulfur batteries, *Adv. Mater.* 29 (2017) 1700587.
- [23] L. Catala, T. Mallah, Nanoparticles of prussian blue analogs and related coordination polymers: from information storage to biomedical applications, *Chem. Rev.* 346 (2017) 32–61.
- [24] N. Zhu, X. Hao, J. Ulstrup, Q. Chi, Single-nanoparticle resolved biomimetic long-range electron transfer and electrocatalysis of mixed-valence nanoparticles, *ACS Catal.* 6 (2016) 2728–2738.
- [25] X. Li, J. Liu, A.I. Rykov, H. Han, C. Jin, X. Liu, J. Wang, Excellent photo-Fenton catalysts of Fe-Co Prussian blue analogues and their reaction mechanism study, *Appl. Catal. B: Environ.* 179 (2015) 196–205.
- [26] M. Avila, L. Reguera, J. Rodríguez-Hernández, J. Balmaseda, Porous framework of T<sub>2</sub>[Fe(CN)<sub>6</sub>]<sub>x</sub>H<sub>2</sub>O with T=Co, Ni, Cu, Zn, and H<sub>2</sub> storage, *J. Solid State Chem.* 181 (2008) 2899–2907.
- [27] J. Sebastian, D. Srinivas, Effects of method of preparation on catalytic activity of Co-Zn double-metal cyanide catalysts for copolymerization of CO<sub>2</sub> and epoxide, *Appl. Catal. A: Gen.* 482 (2014) 300–308.
- [28] R. Srivastava, D. Srinivas, P. Ratnasamy, Fe-Zn double-metal cyanide complexes as novel, solid transesterification catalysts, *J. Catal.* 241 (2006) 34–44.
- [29] P.S. Sreerpranth, R. Srivastava, D. Srinivas, P. Ratnasamy, Solid acid catalysts for production of biofuels and lubricants, *Appl. Catal. A: Gen.* 314 (2006) 148–159.
- [30] M. Kotwal, S.S. Deshpande, D. Srinivas, Esterification of fatty acids with glycerol over Fe-Zn double-metal cyanide catalyst, *Catal. Commun.* 12 (2011) 1302–1306.
- [31] A. Peeters, P. Valvekens, R. Ameloot, G. Sankar, C.E.A. Kirschhock, D.D. Vos, Lewis acid double metal cyanide catalysts for hydroamination of phenylacetylene, *Chem. Commun.* 47 (2011) 4114–4116.
- [32] M.V. Patil, M.K. Yadav, R.V. Jasra, Prins condensation for synthesis of nopol from pinene and paraformaldehyde on novel Fe-Zn double metal cyanide solid acid catalyst, *J. Mol. Catal. A: Chem.* 273 (2007) 39–47.
- [33] A. García-Ortiz, A. Grierrane, E. Reguera, H. García, Mixed (Fe<sup>2+</sup> and Cu<sup>2+</sup>) double metal hexacyanocobaltates as solid catalyst for the aerobic oxidation of oximes to carbonyl compounds, *J. Catal.* 311 (2014) 386–392.
- [34] J.-J. Zou, Y. Xu, X. Zhang, L. Wang, Isomerization of endo-dicyclopentadiene using Al-grafted MCM-41, *Appl. Catal. A: Gen.* 421–422 (2012) 79–85.
- [35] M.S. Kandanapitiye, F.J. Wang, B. Valley, C. Gunathilake, M. Jaroniec, S.D. Huang, Selective ion exchange governed by the Irving-Williams series in K<sub>2</sub>Zn<sub>3</sub>[Fe(CN)<sub>6</sub>]<sub>2</sub> nanoparticles: toward a designer prodrug for Wilson's disease, *Inorg. Chem.* 54 (2015) 1212–1214.
- [36] J. Liu, X. Li, A.I. Rykov, Q. Fan, W. Xu, W. Cong, C. Jin, H. Tang, K. Zhu, A.S. Ganeshraja, R. Ge, X. Wang, J. Wang, Zinc-modulated Fe-Co prussian blue analogues with well-controlled morphology for efficient cesium sorption, *J. Mater. Chem. A* 5 (2017) 3284–3292.
- [37] B.L. Wegenhart, L. Yang, S.C. Kwan, R. Harris, H.I. Kenttämaa, M.M. Abu-Omar, From furfural to fuel: synthesis of furfuroins by organocatalysis and their hydrodeoxygenation by cascade catalysis, *ChemSusChem* 7 (2014) 2742–2747.
- [38] H. Li, J. Chen, Y. Wan, W. Chai, F. Zhang, Y. Lu, Water-medium Ullmann reaction over a highly active and selective Pd/Ph-SBA-15 catalyst, *Green Chem.* 9 (2007) 273–280.
- [39] S. Bhogeswararao, D. Srinivas, Catalytic conversion of furfural to industrial chemicals over supported Pt and Pd catalysts, *J. Catal.* 327 (2015) 65–77.
- [40] M. Samy El-Shall, V. Abdelsayed, A.E. Rahman, S. Khder, H.M.A. Hassan, H.M. El-Kaderi, T.E. Reich, Metallic and bimetallic nanocatalysts incorporated into highly porous coordination polymer MIL-101, *J. Mater. Chem.* 19 (2009) 7625–7631.
- [41] Q. Deng, J. Xu, P. Han, L. Pan, L. Wang, X. Zhang, J.-J. Zou, Efficient synthesis of high-density aviation biofuel via solvent-free aldol condensation of cyclic ketones and furanic aldehydes, *Fuel Process. Technol.* 148 (2016) 361–366.